Simulation of Start-Up Process of Turbofan Engine Based on Full-State Characteristics of Fan

*FANG Jun, ZHANG Tianhong**

College of Energy and Power Engineering, Nanjing University of Aeronautics and Astronautics, Nanjing 210016, P. R. China

(Received 20 May 2024; revised 13 July 2024; accepted 10 August 2024)

Abstract: Difficulties in obtaining component characteristics in the sub-idle state of rotor constrain the simulation capabilities of ground and windmill start-up processes for turbofan engines. This paper proposes a backbone feature method based on conventional characteristics parameters to derive the full-state characteristics of fan. The application of the fan's full-state characteristics in component-level model of turbofan engine enables zero-speed iterative simulation for ground start-up process and windmill simulation for windmill start-up process, thereby improving the simulation capability of sub-idle state during turbofan engine start-up.

Key words: ground start-up simulation; windmill start-up simulation; full-state characteristics; turbofan engine modeling

CLC number: V23 **Document code:** A **Article ID:** 1005-1120(2024)S-0027-08

0 Introduction

Modeling plays a crucial role in the design and development stages of aviation engine[1]. The low-speed state during ground start-up and the windmill state during windmill start-up of aviation engines both fall under the sub-idle state category, which is challenging to simulate using traditional component-level engine model[2]. Obtaining the rotor characteristics in sub-idle state is the key to solving this problem[3].

Currently, many scholars are dedicated to addressing the challenge of simulating sub-idle state of aviation engine. NASA Glenn Research Center proposed a multiple simulation method to tackle the problem of poor convergence in sub-idle state modeling. This method involves modeling steady-state points and transient process transfer functions of sub-idle process to obtain a stable sub-idle state model. When the baseline model encounters non-convergence during sub-idle state, it smoothly switches to the stable sub-idle state model[4]. However, this method does not fundamentally address the issue of obtaining component characteristics in sub-idle state of rotor, limiting its application to windmill start-up simulation only. Recognizing the importance of rotor sub-idle state characteristics, Ref.[5] employed the RANS CFD method to generate zero-speed characteristics of rotor. However, this method depends on precise blade geometry and poses technical challenges. Nowadays, the most used approach to obtain rotor sub-idle state characteristics is analyzing higher-speed rotor characteristics and extrapolating them to low-speed characteristics following a certain pattern. The Sexton method follows this approach and is widely applied due to its simplicity. It derives power function relationships for rotor speed, flow rate, pressure ratio, and efficiency based on similarity principle in pump theory, allowing for low-speed characteristics extrapolation[6]. However, during sub-idle state in aviation engines, the rotor operating point deviates significantly from the design point, leading to unconventional working conditions, such as compressor entering turbine state even at very low speeds[7]. The is-

*Corresponding author, E-mail address: thz@nuaa.edu.cn.

How to cite this article: FANG Jun, ZHANG Tianhong. Simulation of start-up process of turbofan engine based on full-state characteristics of fan[J]. Transactions of Nanjing University of Aeronautics and Astronautics, 2024, 41(S): 27-34.

http://dx.doi.org/10.16356/j.1005-1120.2024.S.004

entropic efficiency of rotor in unconventional working conditions does not fall within the (0,1) range, rendering the Sexton method unable to obtain full-state rotor characteristics. To obtain full-state rotor characteristics, two main methods are currently employed. One involves using converted torque to describe rotor component efficiency characteristics for extrapolation[8], while the other uses the backbone feature method with loss coefficient to describe rotor component efficiency for extrapolation[9-10]. Both methods can be used to extrapolate full-state rotor characteristics.

In both low-speed states during ground start-up and the windmill state during windmill start-up of aviation engines, the fan of the turbofan engine is prone to enter unconventional working conditions[5,11]. Therefore, simulations of the ground start-up process and windmill start-up process require the full-state characteristics of the fan. Although there are existing applications of the backbone feature method for extrapolating rotor full-state characteristics, differences between backbone feature parameters and conventional characteristics parameters pose obstacles in its application. This paper analyzes the physical meaning of backbone feature parameters, establishes a mapping relationship between backbone feature parameters and conventional characteristics parameters, making it easier to extrapolate the full-state characteristics of fan, and finally, validates the simulation of ground start-up process and windmill start-up process.

1 Full-State Characteristics of Fan

The function of fan is to perform work on airflow, converting shaft power into an increase in enthalpy of airflow. Under normal operating conditions, the fan's outlet total pressure is greater than the inlet total pressure, and the outlet total temperature is greater than the inlet total temperature. The isentropic efficiency η of fan can be calculated using Eq.(1), and its efficiency range falls between 0 and 1.

$$\eta=\frac{C_p T_{\text{in}}^*\left(\pi^{\frac{k-1}{k}}-1\right)}{C_p T_{\text{in}}^*\left(T_{\text{out}}^*/T_{\text{in}}^*-1\right)}=\frac{\pi^{\frac{k-1}{k}}-1}{T_{\text{out}}^*/T_{\text{in}}^*-1} \tag{1}$$

where C_p is the specific heat at constant pressure and k the heat capacity ratio; T_{in}^*, T_{out}^* and π refer to the total inlet temperature, the total outlet temperature and the pressure ratio, respectively.

However, when fan operates at lower speeds, its suction and working capabilities decrease significantly. Due to the fan operating far from its design point, severe separation occurs as the airflow passes through the blade passages, resulting in outlet total pressure lower than inlet total pressure. Due to the conversion of kinetic energy loss in the airflow to internal energy, the outlet total temperature is higher than the inlet total temperature. At this point, fan is in a state called stirrer or paddle. When the speed of fan is further reduced, the incoming airflow starts to perform work on fan, causing the fan to enter a state resembling a turbine, with the outlet total pressure lower than the inlet total pressure and the outlet total temperature lower than the inlet total temperature. The differences in isentropic efficiency and inlet/outlet parameters of the fan in various states are summarized in Table 1.

Table 1 Parameter range of fan full-state characteristics

State	Isentropic efficiency	Inlet/Outlet condition
Compressor	$\eta\in(0,1)$	$T_{\text{out}}^*>T_{\text{in}}^*$ $\pi=P_{\text{out}}^*/P_{\text{in}}^*>1$
Stirrer or paddle	$\eta\in(-\infty,0)$	$T_{\text{out}}^*>T_{\text{in}}^*$ $\pi=P_{\text{out}}^*/P_{\text{in}}^*<1$
Turbine	$\eta\in(1,+\infty)$	$T_{\text{out}}^*<T_{\text{in}}^*$ $\pi=P_{\text{out}}^*/P_{\text{in}}^*<1$

When a turbofan engine undergoes ground start-up process, the fan goes through a transition from turbine state to stirrer state and then to compressor state. As shown in Fig.1, in the early stage of the ground start-up process, the starter motor drives the high-pressure shaft rotor to start, and the low-pressure shaft cannot overcome the static friction torque, remaining stationary. The fan operating point starts from the initial point with a pressure ra-

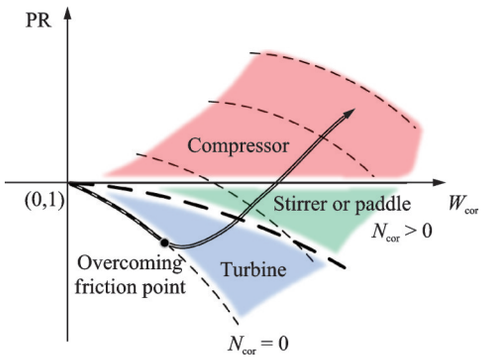

Fig.1 Fan full-state characteristics during ground start-up process

tio (PR) of 1 and zero flow (W_{cor}) along the zero-speed (N_{cor}) line. At this point, the fan is in turbine state. As the high-pressure shaft speed increases, the airflow increases, and the aerodynamic torque on the low-pressure shaft overcomes the static friction torque, causing it to rotate. At this stage, the fan pressure ratio is still less than 1, and the operating point transitions from turbine state to stirrer state. With further acceleration of the low-pressure shaft, the fan's working capability enhances, and the operating point transitions from stirrer state to compressor state.

After an unexpected high-altitude flameout in a turbofan engine, the fan speed rapidly decreases and gradually stabilizes to the windmill speed. However, due to the high flight speed at this time, the decrease in airflow through the fan cannot match the decrease in fan speed. The fan's windmill operating point often falls into the stirrer state or even turbine state, as shown in Fig.2. In the windmill state, the engine can choose between a direct ignition start or assisted start by a starter motor based on its own

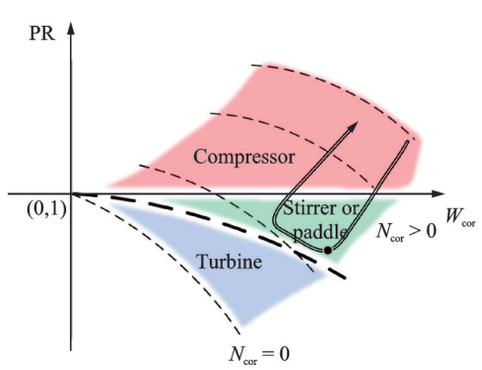

Fig.2 Fan full-state characteristics during windmill start-up process

condition. The fan speed gradually increases, and the operating point transitions from stirrer state or turbine state to compressor state.

In conclusion, the comprehensive analysis above highlights the critical importance of the fan's full-state characteristics in simulating ground start-up process and windmill start-up process. Only by obtaining the fan's full-state characteristics can a more accurate sub-idle start-up model for turbofan engines be established.

2 Backbone Feature Method Based on Conventional Characteristics Parameters

The backbone feature method is an aeroengine rotor characteristics parameterization technique developed in collaboration between General Electric and NASA Lewis Research Center in the 1980s[12-14]. The minimum loss point on each iso-speed line is referred to as the backbone point. The primary concept behind this method is to first extrapolate the low-speed backbone feature based on the existing high-speed backbone feature and then use the extrapolated low-speed backbone feature as a basis for extrapolating low-speed non-backbone feature.

The backbone feature parameters differ from conventional characteristics parameters as they define the flow coefficient φ, the power coefficient ψ, the pressure coefficient ψ_{id}, the loss coefficient C_1, and the virtual Mach number Ma_v to describe rotor characteristics. The differences in parameter definition make it challenging to directly extrapolate rotor sub-idle characteristics using the conventional characteristics parameters through the backbone feature method.

By analyzing the physical meaning of backbone feature parameters, and establishing a mapping relationship between conventional characteristics parameters and backbone feature parameters, it becomes more convenient to apply the backbone feature method based on conventional characteristics parameters. As shown in Table 2, the physical meaning of backbone feature characteristics parameters primarily involves variables such as axial airflow velocity

Table 2 Mapping relationship between backbone feature parameters and conventional characteristics parameters

Backbone feature parameter	Physical meaning	Conventional characteristics parameter mapping
φ	$\frac{V_a}{U}$	$\tilde{\varphi}=\frac{W_{cor}}{N_{cor}}$
ψ_{id}	$\frac{\Delta H_{id}}{U^2/2}$	$\tilde{\psi}_{id}=\frac{\pi^{\frac{k-1}{k}}-1}{N_{cor}^2}$
ψ	$\frac{\Delta H}{U^2/2}$	$\tilde{\psi}=\frac{\pi^{\frac{k-1}{k}}-1}{\eta N_{cor}^2}$
C_l	$\frac{\Delta H-\Delta H_{id}}{U^2/2}$	$\widetilde{C}_l=\frac{\pi^{\frac{k-1}{k}}-1}{N_{cor}^2}\left(\frac{1}{\eta}-1\right)$
Ma_v	$q(Ma)$	$\widetilde{M}a_v=\frac{W_{cor}}{W_{cor,max}}$

V_a, rotor tip speed U, actual enthalpy increase of the airflow after passing through the rotor ΔH, ideal enthalpy increase ΔH_{id}, and virtual Mach number Ma_v.

The axial airflow velocity determines the magnitude of the airflow passing through the rotor, and therefore, the axial airflow velocity can be considered proportional to the corrected flow rate W_{cor}

$$V_a \propto W_{cor} \tag{2}$$

The rotor's tip speed is determined by the rotor's rotational speed. Thus, the rotor's tip speed can be considered proportional to the relative corrected speed N_{cor}

$$U \propto N_{cor} \tag{3}$$

The ideal enthalpy increase of the airflow after passing through the rotor can be calculated using Eq.(4). Since rotor characteristics describe characteristics under similar conditions, $C_p T_{in}^*$ can be considered a constant value. Therefore, the ideal enthalpy increase is related to the conventional characteristic pressure ratio π

$$\Delta H_{id}=C_p T_{in}^*\left(\pi^{\frac{k-1}{k}}-1\right)\propto\pi^{\frac{k-1}{k}}-1 \tag{4}$$

The actual enthalpy increases of the airflow after passing through the rotor needs to account for rotor efficiency and can be described by Eq.(5) to relate the actual enthalpy increase with the pressure ratio π and efficiency η

$$\Delta H \propto \frac{\pi^{\frac{k-1}{k}}-1}{\eta} \tag{5}$$

According to the definition of the virtual Mach number, it is directly proportional to the ratio of corrected flow rate W_{cor} to the maximum corrected flow rate at the same relative corrected speed $W_{cor,max}$

$$Ma_v \propto \frac{W_{cor}}{W_{cor,max}} \tag{6}$$

Based on the above analysis, a mapping relationship between backbone feature parameters and conventional characteristics parameters can be established as described in Table 2.

In furtherance, according to the definition, the point with the minimum loss coefficient mapping parameter $\tilde{C}_l$ on each iso-speed line is identified as the backbone point. A curve is fitted based on the relationship between backbone point mapping parameters and relative corrected speed, and low-speed backbone point mapping parameters are extrapolated from the fitted relationship.

Further extrapolation of non-backbone point mapping parameters is conducted based on backbone point mapping parameters. According to backbone feature method, it is evident that the loss coefficient and flow coefficient approximately exhibit a quadratic relationship, whereas, under ideal conditions, the flow coefficient is linearly related to the power coefficient. Therefore, it can be approximated that the loss coefficient and power coefficient roughly follow a quadratic relationship, which can be described using mapping parameters as

$$\widetilde{C}_l-\widetilde{C}_{l,BB}=\begin{cases}c_1\left|\tilde{\psi}-\tilde{\psi}_{BB}\right|\left(\tilde{\psi}-\tilde{\psi}_{BB}\right) & \tilde{\psi}>\tilde{\psi}_{BB}\\ 0 & \tilde{\psi}=\tilde{\psi}_{BB}\\ c_2\left|\tilde{\psi}-\tilde{\psi}_{BB}\right|\left(\tilde{\psi}-\tilde{\psi}_{BB}\right) & \tilde{\psi}<\tilde{\psi}_{BB}\end{cases} \tag{7}$$

where the subscript BB represents the mapping parameters for backbone points, while no subscript indicates mapping parameters for non-backbone points. Therefore, the extension of C_l only requires fitting the parameters c_1 and c_2 based on the existing non-backbone point mapping parameters.

Since the flow coefficient is linearly related to the power coefficient under ideal conditions, the virtual Mach number is also approximately linearly re-

lated to the power coefficient, which can be described using mapping parameters as

$$\widetilde{M}\, a_{\mathrm{v}} = k\left(\tilde{\psi} - \tilde{\psi}_{\mathrm{BB}}\right) + b \tag{8}$$

By simply fitting the values of k and b, the relationship between the virtual Mach number mapping parameters and the power coefficient mapping parameters can be obtained. Based on the ratio of the virtual Mach number mapping parameters for non-backbone points to those for backbone points, it is easy to determine the ratio of corrected flow for non-backbone points to that for backbone points.

The full-state characteristics of fan obtained through backbone feature method based on conventional characteristics parameters are shown in Fig.3. The low-speed characteristics of fan can reflect turbine state, stirrer state, and compressor state, meeting the characteristic requirements for simulating sub-idle process during start-up of turbofan engine.

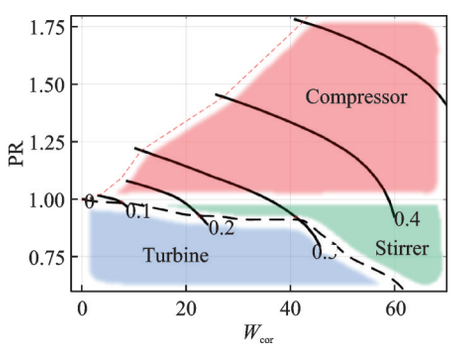

Fig.3 Extrapolation of fan full-state characteristics

3 Simulation of Ground Start-Up Process

During initial stage of turbofan engine start-up process, it is influenced by static friction torque, causing the low-pressure shaft to remain stationary. Therefore, the rotor dynamics equation needs to be rewritten as Eq.(9). Only when low-pressure turbine torque is sufficient to overcome fan torque and static friction torque will the low-pressure shaft begin accelerating from a standstill.

$$J_{\mathrm{L}}\frac{\mathrm{d}n_{\mathrm{L}}}{\mathrm{d}t} = \begin{cases} 0 & T_{\mathrm{LPT}} \leqslant T_{\mathrm{FAN}} + f_{\mathrm{static}} \\ T_{\mathrm{LPT}} - T_{\mathrm{FAN}} - f_{\mathrm{sliding}} & T_{\mathrm{LPT}} > T_{\mathrm{FAN}} + f_{\mathrm{static}} \end{cases} \tag{9}$$

where J_{L} and n_{L} refer to low-pressure shaft rotational inertia and low-pressure shaft rotational speed, respectively; and T_{LPT}, T_{FAN}, f_{sliding} and f_{static} the low-pressure turbine torque, the fan torque, the sliding friction torque, and the static friction torque, respectively.

The flow balance equation for initial stage of turbofan engine start-up process also needs to be modified. When the fan is at low or even zero speed during initial stage, the suction capability of core rotor determines the amount of flow entering the fan. At this point, it can be approximated that the exit flow from the fan is equal to the inlet flow of the high-pressure compressor, like the operation of a turbojet engine. As the fan speed increases, the ability to perform work on the airflow improves. Part of the airflow passes through the core rotor, while the rest goes through the bypass duct, transitioning into the normal operating state of turbofan engine.

The fan's working capability can be reflected by fan pressure ratio, and thus, these two fan states can be switched based on fan pressure ratio π_{FAN}. Define the bypass pressure ratio as π_{BYPASS}, and this parameter' fixed value can be calculated by balancing the outlet static pressure of bypass with the outlet static pressure of low-pressure turbine. Typically, its value falls within the range of 1 to 1.1. As shown in Table 3, when fan pressure ratio is less than the bypass pressure ratio, the fan's working capability is insufficient, and bypass duct is approximated to be inactive. When fan pressure ratio is greater than the bypass pressure ratio, the fan has sufficient compressive action on airflow, and the airflow passing through fan enters both core rotor and bypass duct.

Table 3 Fan flow balance during ground start-up process

Judgment criteria	Fan flow balance	Schematic diagram
$\pi_{\mathrm{FAN}} \leqslant \pi_{\mathrm{BYPASS}}$	$W_{\mathrm{FAN}} = W_{\mathrm{HPC}}$	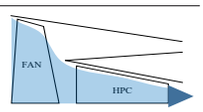
$\pi_{\mathrm{FAN}} > \pi_{\mathrm{BYPASS}}$	$W_{\mathrm{FAN}} = W_{\mathrm{HPC}} + W_{\mathrm{BYPASS}}$	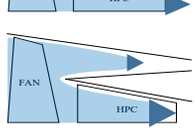

In Table 3, W_{FAN}, W_{HPC} and W_{BYPASS} refer to fan flow, high-pressure compressor flow, and bypass flow, respectively.

Next, a ground start-up process simulation is conducted based on the fan's full-state characteristics. The variation of speed over time during the ground start-up process is shown in Fig.4. In Fig.4, n_H and n_L refer to high-pressure shaft speed and low-pressure shaft speed, respectively. At initial stage, the fan is at zero speed and starts accelerating after about 3 s, overcoming static friction torque. During this time, the fan remains in a turbine state. It is only after ignition that the fan speed further increases, its working capability gradually strengthens, and it transitions from turbine state to stirrer state. Finally, approximately 17 s after starting, the fan enters the normal compressor state.

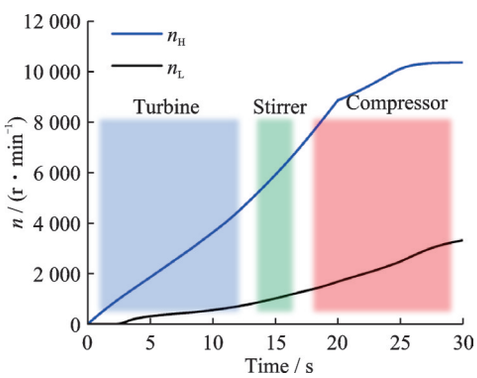

Fig.4 Speed variation during ground start-up process

Fig.5 depicts the changes over time in fan efficiency η, pressure ratio π, power P, and θ the total temperature ratio between outlet and inlet. The variation in fan efficiency provides an intuitive representation of the different states the fan goes through. In both turbine and stirrer states, the fan pressure ratio is less than 1, indicating that the fan has no compression effect on airflow. In turbine state, the fan power

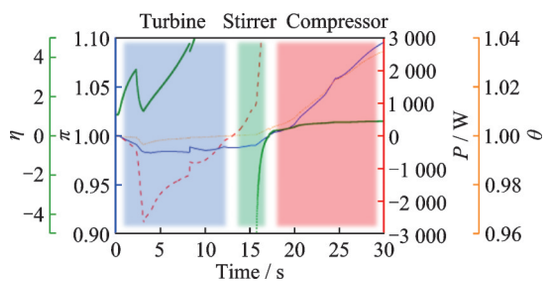

Fig.5 Fan parameter variation during ground start-up process

is negative, suggesting that the fan is, in essence, acting like a turbine, generating power externally. Once it transitions to stirrer state, the fan starts consuming power. In turbine state, the total temperature ratio between outlet and inlet of fan is less than 1, but after entering stirrer state, the outlet total temperature surpasses the inlet total temperature.

The fan operating point trajectory in Fig.6 provides a visual representation of the entire journey that the fan goes through, transitioning from the initial zero-speed state to turbine state, then to stirrer state, and finally to compressor state.

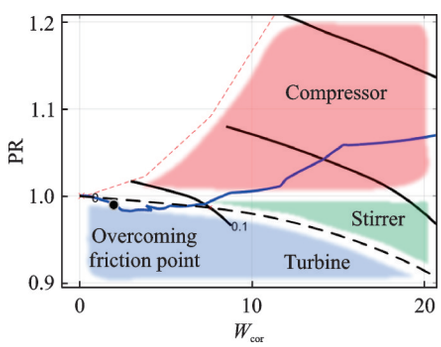

Fig.6 Fan operating point trajectory during ground start-up process

4 Simulation of Windmill Start-Up Process

Simulation of windmill start-up process is conducted at an altitude of 5 km and a Mach number of 1.8. Fig.7 illustrates the change in rotor speed during windmill start-up process, from an unexpected flameout at high altitude to re-ignition and acceleration. At $t=0$, the engine experiences an unexpected flameout, causing a rapid decrease in both high-pressure and low-pressure shaft speeds. The low-pressure shaft speed stabilizes relatively quickly, while

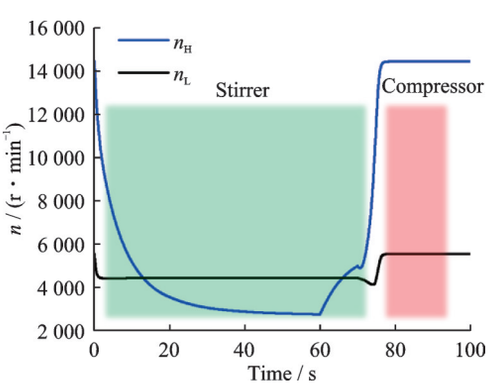

Fig.7 Speed variation during windmill start-up process

the high-pressure shaft speed gradually stabilizes after a more extended period of decrease. After 60 s of the unexpected flameout, the starter engages the high-pressure shaft, igniting the engine when the ignition speed is reached, and the restart acceleration process commences, eventually returning to the original state.

Fig.8 displays the changes over time in fan efficiency η, pressure ratio π, power P, and θ the total temperature ratio between outlet and inlet during windmill start-up process. The variation in fan efficiency reveals that after an unexpected flameout at high altitude, the fan quickly enters stirrer state. The windmill point stabilizes in stirrer state once the fan speed stabilizes. It is only after re-ignition that the fan transitions from stirrer state back to compressor state. The pressure ratio during windmill state remains below 1, and it gradually recovers to the value greater than 1 after windmill start-up. In this scenario, where the fan does not enter turbine state during windmill state, the fan power remains greater than 0, and the fan outlet total temperature is consistently higher than inlet total temperature.

The fan operating point trajectory shown in Fig.9 vividly illustrates the entire journey of the fan

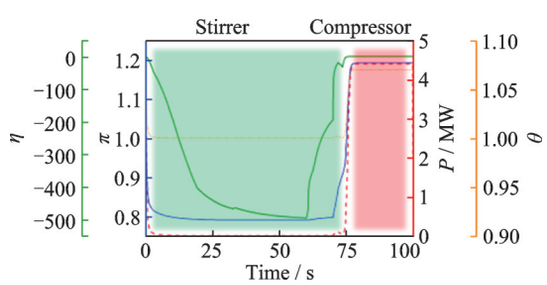

Fig.8 Fan parameter variation during windmill start-up process

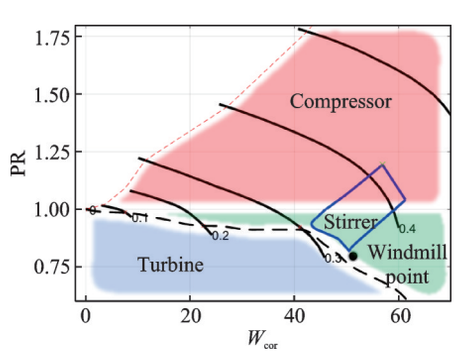

Fig.9 Fan operating point trajectory during windmill start-up process

during the engine's unexpected high-altitude flameout, re-ignition, and restart. It demonstrates how the fan rapidly transitions from compressor state to stirrer state and then back to compressor state during this entire process.

5 Conclusions

To address the simulation challenges of sub-idle processes during ground start-up and windmill start-up for turbofan engines, this paper employs a backbone feature method based on conventional characteristics parameters to obtain the fan's full-state characteristics. Through simulations of ground start-up and windmill start-up processes, the role of fan's full-state characteristics is validated. These characteristics enhance the simulation capabilities of sub-idle process for component-level models of turbofan engines.

Reference

[1] TSOUTSANIS E, LI Y G, PILIDIS P. Part-load performance of gas turbines—Part Ⅱ: Multi-point adaptation with compressor map generation and GA optimization: GTINDIA2012-9581[R]. New York: ASME, 2012.

[2] FUKSMAN I, SIRICA S. Modeling of a turbofan engine start using a high fidelity aero-thermodynamic simulation[C]//Proceedings of ASME Turbo Expo 2012. Copenhagen, Denmark: ASME, 2012.

[3] HAO Wang, WANG Zhanxue, ZHANG Xiaobo. Modeling and simulation study of variable cycle engine windmill starting[J]. Journal of Propulsion Technology, 2022,43(10): 44-54. (in Chinese)

[4] CHAPMAN J W, HAMLEY A J, GUO T, et al. Extending the operational envelope of a turbofan engine simulation into the sub-idle region: NASA/TM-2016-219110[R]. [S.l.]: NASA, 2016.

[5] FERRER-VIDAL L E, IGLESIAS-PÉREZ A, PACHIDIS V. Characterization of axial compressor performance at locked rotor and torque-free windmill conditions[J]. Aerospace Science and Technology, 2020, 101: 105846.

[6] SEXTON W R. A new method to control turbofan engine starting by varying compressor surge valve bleed[D].Blacks burg, Virginia State,USA: Virginia Polytechnic Institute and State University,2001.

[7] ZACHOS P K. Gas turbine sub-idle performance modelling altitude relight and windmilling[D]. England,

UK: Cranfield University, 2010.

[8] ZHANG Mingyang, WANG Zhanxue, ZHANG Xiaobo. Simulation of windmilling-ram mode performance for tandem TBCC engine[J]. Journal of Aerospace Power, 2018, 33(12): 2939-2949. (in Chinese)

[9] WANG Jiamei, GUO Yingqing, YU Huafeng. Extension method of engine low speed characteristics based on backbone features[J]. Journal of Beijing University of Aeronautics and Astronautics, 2022,49(9): 2351-2360. (in Chinese)

[10] SHI Yang, TU Qiuye, YAN Hongming. A full states performance model for aero engine[J]. Journal of Aerospace Power, 2017, 32(2): 373-381. (in Chinese)

[11] BRETSCHNEIDER S, REED J. Modeling of start-up from engine-off conditions using high fidelity turbofan engine simulations[J]. Journal of Engineering for Gas Turbines and Power, 2016. DOI: 10.1115/1.4031474.

[12] CONVERSE G L, GIFFIN R G. Extended parametric representation of compressor fans and turbines. Volume 1: CMGEN user's manual: NASA-CR-174645[R]. Cincinnati, Ohio: Aircraft Engine Business Group, 1984.

[13] CONVERSE G L. Extended parametric representation of compressor fans and turbines. Volume 2: Part user's manual: NASA-CR-174646[R]. Cincinnati, Ohio: Aircraft Engine Business Group, 1984.

[14] CONVERSE G L. Extended parametric representation of compressor fans and turbines. Volume 3: MOD-FAN user's manual: NASA-CR-174647[R]. Cincinnati, Ohio: Aircraft Engine Business Group, 1984.

Acknowledgement This work was supported by Science Center for Gas Turbine Project (No.P2023-B-V-001-001).

Authors Mr. **FANG Jun** received his B.Sc. degree from Nanjing University of Aeronautics and Astronautics in 2020. Now, he is a doctoral student in Nanjing University of Aeronautics and Astronautics. His primary research focus is on modeling and control of multi-electric aeroengines.

Dr. **ZHANG Tianhong** received his Ph.D. degree from Nanjing University of Aeronautics and Astronautics in 2001. He primarily engages in teaching and scientific research in the fields of gas turbine engine control, simulation, and testing technologies, and is committed to the engineering application research of advanced theory and methods. He has undertaken dozens of national special projects, won six provincial and ministerial-level awards, published more than 100 academic papers, obtained more than 40 authorized invention patents.

Author contributions Mr. **FANG Jun** carried out major research work, including engine modeling and simulation, simulation data organization and drawing, and writing paper drafts. Dr. **ZHANG Tianhong** provided the research ideas for the paper, provided guidance on the problems encountered during the modeling process, and suggested revisions to the draft of the paper. The authors commented on the manuscript draft and approved the submission.

Competing interests The authors declare no competing interests.

(Production Editor: SUN Jing)

基于风扇全状态特性的涡扇发动机起动过程仿真

方 鋆，张天宏

(南京航空航天大学能源与动力学院，南京 210016，中国)

摘要：转子慢车以下状态部件特性难以获得制约了涡扇发动机地面起动过程和高空起动过程的仿真能力。本文针对风扇特性提出采用基于常规特性参数的脊背法，外推得到风扇全状态特性。应用风扇全状态特性的涡扇发动机部件级模型在地面起动过程仿真中实现零转速迭代仿真，高空起动过程实现风车状态仿真，提高了涡扇发动机起动过程慢车以下状态的仿真能力。

关键词：地面起动仿真；高空起动仿真；全状态特性；涡扇发动机建模